The running kinematics of free-roaming giraffes, measured using a low cost unmanned aerial vehicle (UAV)

Christopher K Basu [Corresp., 1] , Francois Deacon [2] , John R Hutchinson [1] , Alan M Wilson [1]

[1] Structure & Motion Laboratory, Royal Veterinary College, Hatfield, United Kingdom

[2] Faculty of Natural and Agricultural Sciences, Department of Animal, Wildlife and Grassland Sciences, University of the Free State, Bloemfontein, South Africa

Corresponding Author: Christopher K Basu
Email address: cbasu@rvc.ac.uk

The study of animal locomotion can be logistically challenging, especially in the case of large or unhandleable animals in uncontrolled environments. Recent technological advances have permitted the use of Global Positioning System and inertial sensors in locomotion studies, but these methods require manual access to each study subject. Here we demonstrate the utility of a low cost unmanned aerial vehicle (UAV) in measuring two-dimensional running kinematics from free-roaming giraffes (*Giraffa camelopardalis giraffa*) in the Free State Province, South Africa. We collected 120 Hz video of running giraffes, and calibrated each video frame using metatarsal length as a constant object of scale. We tested a number of methods to measure metatarsal length. The method with the least variation used close range photography and a trigonometric equation to spatially calibrate the still image, and derive metatarsal length. In the absence of this option, a spatially calibrated surface model of the study terrain was used to estimate topographical dimensions in video footage of interest. Data for the terrain models were collected using the same equipment, during the same study period. We subsequently validated the accuracy of the UAV method by comparing similar speed measurements of a running human subject, with a gold standard method. We recommend that future users maximise the camera focal distance, and keep the subject in the central field of view.

The studied giraffes used a grounded rotary gallop with a speed range of 3.4 to 6.9 ms^{-1} (never cantering, trotting or pacing), and lower duty factors when compared with other cursorial quadrupeds. As this pattern might result in adverse increases in peak vertical limb forces with speed, it was notable to find that contralateral limbs became more in-phase with speed. Considering the latter pattern and the modest maximal speed of giraffes, we speculate that tissue safety factors are maintained within tolerable bounds this way. Furthermore, the angular kinematics of the neck were frequently isolated from the pitching of the body during running; this may be a result of the large mass of the head and neck. Further field experiments and biomechanical models are needed to robustly test these speculations.

1 **The running kinematics of free-roaming giraffes, measured using a low cost**
2 **unmanned aerial vehicle (UAV)**

3 Christopher K. Basu[1], Francois Deacon[2], *John R. Hutchinson[1], *Alan M. Wilson[1]
4
5 [1] Structure & Motion Laboratory, Royal Veterinary College, Hatfield, Hertfordshire, UK
6 [2] Faculty of Natural and Agricultural Sciences, Department of Animal, Wildlife and Grassland
7 Sciences, University of the Free State, Bloemfontein, Republic of South Africa
8
9 Corresponding Author:
10 Christopher Basu
11 Royal Veterinary College, Hatfield, Hertfordshire, AL9 7TA, UK
12 Email address: cbasu@rvc.ac.uk
13
14 * Co-senior authors
15

ABSTRACT

17 The study of animal locomotion can be logistically challenging, especially in the case of large or

18 unhandleable animals in uncontrolled environments. Recent technological advances have

19 permitted the use of Global Positioning System and inertial sensors in locomotion studies, but

20 these methods require manual access to each study subject. Here we demonstrate the utility of a

21 low cost unmanned aerial vehicle (UAV) in measuring two-dimensional running kinematics

22 from free-roaming giraffes in the Free State Province, South Africa. We collected 120 Hz video

23 of running giraffes, and calibrated each video frame using metatarsal length as a constant object

24 of scale. We tested a number of methods to measure metatarsal length. The method with the least

25 variation used close range photography and a trigonometric equation to spatially calibrate the

26 still image, and derive metatarsal length. In the absence of this option, a spatially calibrated

27 surface model of the study terrain was used to estimate topographical dimensions in video

28 footage of interest. Data for the terrain models were collected using the same equipment, during

29 the same study period. We subsequently validated the accuracy of the UAV method by

30 comparing similar speed measurements of a running human subject, with a gold standard

31 method. We recommend that future users maximise the camera focal distance, and keep the

32 subject in the central field of view. The studied giraffes used a grounded rotary gallop with a

33 speed range of 3.4 to 6.9 ms^{-1} (never cantering, trotting or pacing), and lower duty factors when

34   compared with other cursorial quadrupeds. As this pattern might result in adverse increases in

35   peak vertical limb forces with speed, it was notable to find that contralateral limbs became more

36   in-phase with speed. Considering the latter pattern and the modest maximal speed of giraffes, we

37   speculate that tissue safety factors are maintained within tolerable bounds this way. Furthermore,

38   the angular kinematics of the neck were frequently isolated from the pitching of the body during

39   running; this may be a result of the large mass of the head and neck. Further field experiments

40   and biomechanical models are needed to robustly test these speculations.

41

42

INTRODUCTION

Measuring gait parameters outside of the laboratory

Biomechanical measurements of animal locomotion are commonly performed under laboratory conditions. Under these circumstances, confounding variables may be measured and/or controlled. When studying animals, particularly undomesticated animals usually living in natural habitats, the laboratory itself can become a confounding variable. Natural behaviours are less likely to be expressed, and it is difficult to replicate the interactions between the animal and its natural environment (e.g. temperature, light, substrate properties). In many cases it is not logistically possible or safe to study animals in a laboratory setting.

In recent years, the increasing availability of remote sensing has broadened the focus of locomotor research to include more field-based data collection. Accelerometers and Global Positioning System (GPS) devices have been used to derive three-dimensional temporospatial parameters in a variety of human (Tao et al. 2012) and non-human locomotor studies (Daley et al. 2016; Hubel et al. 2016). Whilst these methods are an excellent solution to study locomotor behaviours over an extended period of time, one challenge is that physical access to each study subject is required. This inevitably requires an instance of either manual or chemical restraint.

If two-dimensional (2D) temporospatial kinematics are required, a low cost alternative is to use an unmanned aerial vehicle (UAV) to gather spatially calibrated video footage of the locomotor behaviour in question. In this study, we demonstrate the utility of a single low-cost UAV in measuring the 2D kinematic gait parameters of free-ranging running giraffes (*Giraffa camelopardalis giraffa*). We use these data to question whether giraffes' running gait is specialised when compared with other mammalian quadrupeds.

Gait dynamics in giraffes and other quadrupedal mammals

Quadrupeds typically use asymmetrical gaits at faster speeds. In asymmetrical gaits the fore- and hindfeet each act as functional pairs, where each pair of feet can strike the ground simultaneously, or may have a time lag between the footfall of the left and right side, in which case there is a leading and a trailing foot. Galloping gaits may be further defined by the pattern of the leading limbs. In a transverse gallop, the leading limbs of the fore and hind quarters are on the same side of the body, *versus* a rotary gallop where the leading limbs are on the opposite

72   sides of the body. In either case, both a gathered and extended aerial phase can be present, where

73   all feet are airborne (Hildebrand, 1977, Biancardi and Minetti, 2012).

74   At walking speeds, giraffes use a lateral sequence walk, which is dynamically similar to the slow

75   gaits of other mammalian quadrupeds (Basu et al. Under review). The theory of dynamic

76   similarity predicts that geometrically similar animals move with similar dimensionless stride

77   parameters at equivalent dimensionless speeds. Dimensionless speed is expressed here as Froude

78   number (Eqn 1), where u = speed (ms^{-1}), h = shoulder height (m) and g = acceleration due to

79   gravity (9.81 ms^{-2}).

80    $$Fr = \frac{u^2}{gh}$$ Eqn 1

81   Giraffes appear to diverge from the predictions of dynamic similarity at faster than walking

82   speeds. Instead of using an intermediate speed gait, such as a trot, giraffes seemingly transition

83   consistently from a walk to a rotary gallop (Dagg & Vos 1968; Maxwell 1924). The restricted

84   choice of gait is in contrast to most other cursorial quadrupeds (Heglund & Taylor 1988;

85   Hildebrand 1976), but not exclusive to giraffes; for example elephants use the lateral sequence

86   walk across their entire speed range (Hutchinson et al. 2006). At near-maximal running speeds,

87   giraffes are thought to use lower mean stride frequencies (and consequently higher stride

88   lengths) than is expected for an ungulate of their body mass; an ability that may be facilitated by

89   their elongate limbs (Alexander et al. 1977).

90   Giraffes' long neck may have functional consequences with respect to the locomotor system.

91   Evolutionary elongation of giraffes' cervical vertebrae has effectively lengthened their horizontal

92   axis (Badlangana 2009). In other galloping quadrupeds, the horizontal axis of the skeleton is

93   dynamic, where fluctuations in neck angle and body pitch occur during walking and running

94   (Dunbar 2004; Dunbar et al. 2008). Such angular fluctuations may serve to stabilise these axial

95   body segments in world space. In giraffes, Dagg noted the periodic angular fluctuations of the

96   neck, and found this to be larger in magnitude during the gallop than in the walk (Dagg 1962).

97   One way to define this effect of neck and pitching angles on the horizontal axis is to determine

98   the phase relationship between the kinematics of the trunk and the neck (Basu et al. Under

99   review).

100   Our aims in this study are to (1) validate the use of a UAV in measuring temporospatial gait

101   parameters and suggest recommendations for optimising data quality; (2) determine which

102 running gait(s) the giraffes select across their speed range, (3) determine how stride parameters

103 change within the running gait, (4) assess whether giraffes' running gait is specialised compared

104 to other cursorial quadrupeds, and finally (5) measure the angular kinematics of the neck and

105 body, and predict how their phase relationship contributes to body segment stability.

106

107

108 MATERIALS & METHODS

109 Video data of giraffes' running gait were recorded from three field sites in the Free State

110 Province, South Africa. A total of 35 giraffes were available for study; these varied in age, size

111 and sex (Table 1). The experimental protocol varied between the field sites, and was dependent

112 on the giraffes' degree of familiarity with people. A Phantom 4 UAV (DJI, Guangdong, China)

113 was used to film giraffes' locomotion from a lateral viewpoint, at 120 Hz, 1920 x 1080 pixel

114 resolution, with a 20 mm lens. This was the maximum possible frame rate and image resolution

115 of any low-cost UAV (<£1000) at the time the study was conducted.

116 The giraffes were motivated to run using different methods. In field site 1 (Table 1), giraffes

117 were accustomed to following a vehicle as part of their usual routine. During data collection, a

118 vehicle was driven along a straight track at steady speed. A 200 m segment of this track was

119 outlined with white paint marks spaced at 2 m intervals. This speed of the vehicle was

120 periodically varied to induce different steady state running speeds. In field sites 2 and 3, the

121 giraffes were less habituated to humans and vehicles; in these sites the sound and proximity of

122 the UAV was sufficient to induce galloping for short distances.

123 **Ethical statement**

124 This study had ethical approval from both the Royal Veterinary College (URN 2016 1538) and

125 the University of the Free State, South Africa (UFS-AED2016/0063). A regional permit to study

126 giraffes was obtained from the Department of Economic Development, Tourism and

127 Environmental Affairs (DEDTEA, Free State Province, South Africa) was obtained (permit

128 number 01/34481). Data were gathered during a two week period in October 2016; that month

129 was chosen as it was during the dry season, and typically lacks the extreme low and high

130 temperatures seen at other times of the year. Measures were taken to minimise stress and danger

131 to the giraffes, and management personnel were present at each site at all times. Firstly, data

132 were gathered during cooler times of day to minimise the risk of heat stress. Secondly, giraffes

133   were only filmed in open habitats with minimal ground obstructions. Thirdly, individual giraffes

134   were only motivated to run up to twice daily, and for sustained periods of time less than one

135   minute. In between bouts of data collection, giraffes were allowed to express normal behaviour.

136

137   **Video calibration**

138   Prior calibration of UAV mounted cameras is not possible, as the subject-to-camera distance is

139   not constant as it is with a static camera. Three calibration methods were used, either in

140   combination or isolation (Table 1). With each method, the distance from the metatarsophalangeal

141   joint to the most caudal point of the calcaneus (MTP-C; Figure 1) was used to calibrate each

142   frame of digitised video. The MTP joint centre was measured as the centroid of a circle drawn

143   around the joint. Video footage was manually digitised using the DLTDV6 (Hedrick 2008) script

144   for Matlab (MathWorks Inc., Natick, MA, USA) software, using a system of virtual markers

145   (Basu et al., Under review). The giraffes' natural coat patterns were used to maximise

146   digitisation repeatability.

147   The MTP-C distance was measured using method A, B or C. Method A used close range digital

148   photography and a trigonometry calculation (Eqns 2 to 4) to estimate the size of MTP-C.

149   Photographs (Canon EOS 500D, 18-200 mm 5.6f lens, Tokyo, Japan) were opportunistically

150   taken of each giraffe, focusing on the hindlimb. For each photograph, the distance from the

151   camera sensor to the subject's area of interest was measured using a laser rangefinder (Disto D5,

152   Leica, Wetzlar, Germany), and the lens focal length was later retrieved from the image metadata.

153    $horizontal\ angle\ of\ view\ (°) = 2 * \text{atan} \left(\frac{sensor\ size}{2 * focal\ length} \right)$ Eqn 2

154    $horizontal\ field\ of\ view\ (m) = 2 * distance * \tan \left(\frac{angle\ of\ view}{2} \right)$ Eqn 3

155    $photo\ calibration\ constant = \frac{horizontal\ field\ of\ view\ (m)}{number\ of\ horizontal\ pixels}$ Eqn 4

156

157   The pixel MTP-C distance was then measured in each photograph using ImageJ (Rasband 2009),

158   and converted to estimated metric distance using the calibration constant from Eqn 4. This

159   trigonometry method assumes that the camera sensor is perpendicular to the subject. It was not

160   possible to quantitatively measure the optical axis of the camera; therefore, parallax errors may

161   have affected the resulting calculations. To offset this error, the mean estimate was used to

162   calibrate video footage. Due to the close-range nature of the photographs, this method was only

163   suitable in field site 1, which had a more controlled and predictable environment.

164   In Method B, 2 m ground markers were used to calibrate 10 still frames from video footage of

165   each giraffe, as they moved parallel with the markers. MTP-C distance was estimated from these

166   frames, and the mean value used to calibrate subsequent video data. This method was only

167   possible in field site 1, where the giraffes could be led along the 200 m track.

168   Method C was used where the giraffes' locations and locomotion trajectories could not be

169   anticipated (field sites 2 and 3). After recording video data, a textured 3D mesh of the terrain was

170   produced using aerial photographs taken from the UAV during an aerial survey at 40 m altitude.

171   The derived models were created using the software package Pix4D (Lausanne, Switzerland),

172   which takes GPS stamped photographs as an input, and outputs scaled and textured 3D meshes

173   of the corresponding terrain, using a photogrammetry method. These models were used to

174   identify and measure prominent ground features, which could be cross-referenced with features

175   in digitised video, and subsequently used to measure MTP-C distance. The criteria for suitable

176   ground features were that they had to be within the sagittal plane of the giraffe, and be

177   distinguishable on the 3D mesh and the video (Figure 1).

178   **Kinematic data processing**

179   Footage from statically mounted videos has a fixed coordinate system, originating from one

180   corner of the video. Footage from a moving camera has no fixed coordinate system, as the

181   boundaries of the video change with each frame. To compensate for this, an in-plane static

182   ground point was digitised for each analysed stride, and the digitised coordinates translated

183   relative to this fixed point. Rotational transformation of digitised points was not performed, as

184   camera rotation during flight was corrected by a three-axis stabilised gimbal, which corrects the

185   pitch, yaw and roll of the camera to the nearest 0.02° (https://www.dji.com/phantom-4-pro/info).

186   This experimental setup allowed for a single lateral camera view. A consequence was that far

187   side foot-on events frequently were obscured; however far side foot-off events reliably were

188   visible. These data allowed contralateral limb phase (the lag between a pair of fore or hindlimb

189   footfalls) to be measured, however ipsilateral limb phase (the lag between fore and hind

190   footfalls) could not be measured, as this requires the foot on and off timings for all four feet to be

191   measured (Hildebrand 1977). The complete set of foot events were visible in one stride, which

192   was used to quantify the footfall sequence for the galloping gait. We defined a stride by the

193   timing from the nearside hindlimb foot-ground contact event, to the timing of the subsequent

194   nearside hindlimb foot event.

195   A number of criteria were used to ensure that stride data were suitable for analysis. An

196   assumption of linear regression is that the data units are independent from each other. To ensure

197   that this assumption was met, only one stride from a sequence of consecutive strides was used in

198   the analyses. A sequence of consecutive strides was defined as being bounded by either a change

199   in gait, or an obvious change in steady state speed. Only steady-state strides were analysed;

200   strides which featured a 20% or greater change in speed over their course were excluded. Speed

201   was subsequently measured as the horizontal displacement of the giraffes' withers over the

202   course of one stride (m), divided by the time interval (s).

203   Strides were manually segmented with a user-based determination of foot timings. Ideally a

204   velocity threshold method provides a repeatable method of detecting foot contact events (Starke

205   & Clayton 2015), but could not be used in this instance due to excessive measurement noise. A

206   custom-written Matlab script then applied the pixel calibrations and transformations to the raw

207   data. The following parameters were calculated: running speed (ms^{-1}), stride length (m), stride

208   frequency (Hz), footfall timings, contralateral limb phase (the fraction of the stride between

209   footfalls of leading and non-leading limbs), stride duration (s), stance duration (s), duty factor

210   (the fraction of the stride that a given foot is in contact with the ground), neck angle and body

211   pitch angle (°).

212   The phase relationship between neck angle and body pitch was calculated as the percent

213   congruity. This is a measure of how often the slopes of neck angle and body pitch time series

214   share the same sign; indicating whether the respective angular patterns of the neck and body are

215   in-phase (high congruity) or out-of-phase (low congruity) (Ahn et al. 2004). Using the angle

216   convention defined in Figure 2A, 100% congruity represents simultaneous neck ventroflexion

217   and 'motor-bike' body pitching, whilst 0% represents simultaneous neck dorsiflexion with

218   upward body pitching.

219   **Comparisons with dynamic similarity**

220   Power equations were determined to fit Froude number to relative stride length (stride length/ leg

221   length), fore duty factor and hind duty factor. Plotted data from Figures 3 and 4 of Alexander and

222   Jayes (1983) were digitised using a web based application

223   (http://arohatgi.info/WebPlotDigitizer), and power curves were fitted to the resulting data, to test

224   how well our giraffe data fit those data for other mammals. The 95% confidence intervals of the

225   exponents and coefficients from the current dataset were compared with the corresponding

226   intervals from Alexander and Jayes' models of dynamic similarity (Alexander & Jayes 1983).

227   **Statistical analysis of stride parameters**

228   Statistical procedures were carried out using the Matlab Statistical Toolbox. All stride

229   parameters were tested for normality using a Kolmogorov-Smirnov test. Differences in fore or

230   hindlimb parameters were identified using a two-tailed t-test, and analysed separately if

231   statistically significant differences were present. OLS linear regressions were performed using

232   speed as the independent variable, and stride and force parameters as the dependant variable. To

233   compensate for multiple statistical comparisons, critical p-values were adjusted using the

234   Benjamini-Hochberg procedure, using a false discovery rate of 0.05 (Benjamini & Hochberg

235   1995).

236   **Method comparison and validation**

237   The precision of speed measurements was dependent on the precision of the MTP-C

238   measurements, i.e. the calibration method. The three calibration methods were compared in field

239   site 1, using one giraffe. In the case of method C, MTP-C distance was estimated separately

240   using both the artificial ground markers ($C_{ARTIFICIAL}$), and naturally occurring features

241   ($C_{NATURAL}$).

242   Method A (using close range photography) subsequently had the lowest standard deviation

243   between ten repeated measurements, and was used to quantify the percentage error of the other

244   methods:

245   Percentage error of Method$_{OTHER}$ $= \dfrac{Estimate_{OTHER} - Estimate_{A}}{Estimate_{A}} * 100$ Eqn 5

246   We assessed the accuracy of UAV derived measurements of speed in a separate validation study,

247   based on Method A. The field conditions were approximated by measuring the speed of a human

248   subject as they ran on a treadmill. Written consent from the human participant was obtained.

249 Prior to the experiment, the subject's knee to ankle distance was measured using close range

250 photography and Eqns 2 to 4. Skin markers overlying the lateral femoral condyle and lateral

251 malleolus were used to aid digitisation, and the treadmill belt was marked in 0.5 m increments.

252 The speed of the treadmill belt was used as the 'gold standard' to which UAV derived speeds

253 were compared. Treadmill speed was measured using marker displacement (m) divided by time

254 (s). Subject speed was separately measured as in Method A, using a point on the subject's chest

255 and the treadmill belt markers to measure displacement. Each frame of video data was calibrated

256 using the subject's knee to ankle distance.

257 We performed trials under three conditions, where the focal distance and camera axis were

258 independently varied. In each condition, the subject was instructed to run through their

259 comfortable speed range on a treadmill. The treadmill speed was adjusted accordingly in stages.

260 In the first condition the Phantom 4 UAV was manually held (i.e. without a fixed support) at a

261 distance of 4 m from the subject, and for the second condition at 8 m distance. In both these

262 conditions the camera's axis was centred on the subject. In the third condition, the focal distance

263 was kept at 4 m, but the camera's focal axis was offset laterally so that the subject was recorded

264 in the lateral third of the camera's field of view. This final condition explicitly tested the effect of

265 parallax distortion on data accuracy.

266 Percentage error (Speed$_{ERROR}$) was defined from the gold standard measurements of speed

267 (Speed$_{GOLD}$) and measurements derived from the UAV (Speed$_{UAV}$):

268 $$Speed_{ERROR} = \frac{Speed_{GOLD} - Speed_{UAV}}{Speed_{GOLD}} \times 100 \qquad\qquad \text{Eqn 6}$$

269 We then tested the effects of camera focal distance and axis offset on percentage error, using a

270 two-way ANOVA.

271

RESULTS

273 Over 50 stride sequences were filmed, where the body and footfalls of at least one giraffe where

274 clearly visible. Data from 25 representative strides from four similarly-sized adult individuals

275 were included in the analysis (e.g. Video S1).

276 **Method comparison and validation**

277 Close range photography (Method A) yielded MTP-C estimates with the lowest standard

278 deviation (Table 2), and was used to estimate percentage error for Method B and C. The

279 percentage error of method B was 3.7%, with a 4 mm higher standard deviation than Method A.

280 When Method C (using a GPS calibrated terrain model) was applied using the artificial markers,

281 the percentage error was also 3.7%. The percentage error (5%) and standard deviation (0.1 m)

282 was larger when natural ground features ($C_{NATURAL}$) were used. Method A was subsequently

283 used to calibrate footage from field site 1, and method $C_{NATURAL}$ was used for sites 2 and 3.

284 We compared speeds measured using a UAV with a gold standard method, using a human

285 running on a treadmill. Speeds measured with the UAV were consistently lower than treadmill

286 speed. Across all the experimental conditions, the mean measurement error was 13% of treadmill

287 speed. The condition with the highest mean error was condition 3 (focal distance of 4 m with an

288 offset axis) with an error of 17%; and the lowest was condition 2 (focal distance of 8 m), with an

289 error of 8%. Both camera focal distance and axis offset resulted in significant differences in

290 $Speed_{ERROR}$ (ANOVA $p < 0.0001$ and $p = 0.04$ respectively), with distance having the largest

291 effect (Figure 3).

292 **Giraffe running kinematics**

293 The observed speeds ranged from 3.4 to 6.9ms^{-1}, with a mean of 5 ms^{-1} (or Fr 1.35). Given that

294 the individuals studied were of similar size, absolute speeds were analysed. Giraffes moving

295 immediately slower than this speed range used the lateral sequence walking gait, consistent with

296 previous observations in giraffes (Basu et al., under review). In the adult giraffes studied, the

297 observed running gait was a grounded rotary gallop (Figure 4). Brief aerial phases were only

298 observed in juveniles, and are not covered in the present analysis.

299 Linear regression results are reported in Table S1. A statistically significant increase in stride

300 length ($p<0.001$) and stride frequency ($p<0.001$) was observed (Figure 5), respectively

301 representing an increase of 0.5 m and 0.05 Hz for each 1 ms^{-1} increase in speed. Stance duration

302 (Figure 6A) was greater in the forelimb compared with the hindlimb ($p<0.001$), and decreased

303 with speed ($p<0.001$). In contrast, swing duration (Figure 6B) was shorter in the forelimb versus

304 the hindlimb ($p<0.001$). There was however, no observed relationship between swing duration

305 and speed ($p = 0.8$). Duty factors (Figure 6C) and contralateral limb phase (Figure 7) decreased

306   with speed (p < 0.001 and p = 0.002 respectively), and were greater in the forelimb (p<0.001 for

307   both parameters).

308   The body pitch fluctuation resembled a sine wave, and cycled once throughout the stride (Figure

309   2C), with an increase in pitching coinciding with the foot-off events of the forelimbs. The neck

310   angle oscillated once throughout the stride, although the pattern of change was more irregular

311   and more variable between strides (Figure 2B) than the body pitch angle. Neck range of motion

312   and body pitching did not vary as a function of speed (p = 0.68 and 0.07 respectively). Neck

313   angle and body pitch had a mean percent congruity of 70% (standard deviation 18%).

314   **Dynamic similarity**

315   Table 3 summarises the equations that describe how relative stride length and duty factors

316   changed with dimensionless speed in running giraffes. The coefficients and exponents were

317   compared with the predictive equations for dynamic similarity (Alexander & Jayes 1983).

318   Relative stride length in giraffes was consistent with these predictions. The coefficients (*a*)

319   describing 'duty factor versus speed' in giraffes were significantly lower than expected from the

320   models for dynamic similarity.

321

322

323   # DISCUSSION

324   This study has highlighted the potential gains of using a UAV to collect field-based kinematics.

325   Using a moving *vs.* static camera allowed for a larger quantity of data to be recorded than would

326   otherwise have been possible. We have shown that speed and other 2D kinematic parameters can

327   be measured in this way. The major technical challenge was calibrating the raw footage to

328   calculate spatial parameters. The most consistent calibrations were gained when the study subject

329   was close enough to take repeated photographs, or when artificial markers were included in the

330   field of view. We tested the accuracy of this UAV method, and found that speed accuracy was

331   optimised at a longer focal distance, and when the subject was centred in the field of view

332   (Figure 3). Both of these conditions minimise the effect of parallax error on spatial

333   measurements (distances and angles). In addition to minimising error, long focal distances are

334   preferred to minimise potential stress to animal subjects. As a general rule, we recommend that

335   subjects are confined at least to the centre block of a 3x3 grid in the field of view (Figure 8),

336   whilst recognising the trade-off between focal distance and image resolution.

337   When close range photography or artificial ground markers are not feasible, a detailed 3D

338   textured mesh of the terrain may be used to calibrate the images, but this method resulted in an

339   additional calibration error of 5% (Table 2). An error of this magnitude does not alter our

340   findings about giraffe kinematics, but should be considered for future studies. The additional

341   error is related to the subjectivity of picking terrain landmarks which are visible in both the video

342   and 3D mesh. It is important that clearly visible ground features are used; this was illustrated by

343   the difference in error between using artificial ground markers *versus* naturally occurring

344   features (Table 2). A means to address this in future would be to increase the texture resolution

345   of the 3D mesh, to aid in identifying ground points. This can be done by conducting the aerial

346   survey closer to the ground, but as a trade-off, this demands more images per area, resulting in

347   longer flight times. As UAV battery life improves, this trade-off will become less important.

348   Camera sampling rate was also a limitation. 120 Hz was the standard for low-cost UAV

349   technology at the time of data collection. Whilst this was sufficient for measuring displacement

350   and speed across the stride, measuring the velocity or acceleration during foot contact events (for

351   the purpose of stride segmentation) resulted in excessive noise. In future, an interpolation

352   approach could be used to artificially increase the sampling rate.

353   Using this methodology, we were able to measure temporospatial parameters in free-roaming

354   giraffes without any physical contact. We found that giraffes' lack of an intermediate speed gait

355   (e.g. trot/pace) was compensated for by their rotary galloping gait, in that the walk-gallop

356   transition speed of approximately 3.4 ms^{-1} fell close to the mass-specific minimum trotting speed

357   observed in other mammalian quadrupeds (Heglund & Taylor 1988). For example, using Eqn 7,

358   a giraffe weighing 700 kg would be expected to have a minimum trotting speed of 3 ms^{-1}.

359   Minimum trotting speed = 0.593(body mass$^{0.249}$)   Eqn 7

360   In absolute terms, giraffes can be thought of as being slow gallopers (without routinely using a

361   cantering gait). Beyond the walk-to-gallop transition, increases in galloping speed were almost

362   exclusively achieved by increases in stride length; contrasting with the conserved range of stride

363   frequencies. This pattern is consistent in a wide range of quadrupedal running animals, and is

364   thought to reduce mass-specific energy costs (Heglund & Taylor 1988).

365   The giraffes in this study galloped with lower duty factors than predicted by dynamic similarity

366   (Table 3). It is tempting to suggest that giraffes experience similarly higher than expected

367   vertical peak ground reaction forces (GRFs) at equivalent speeds, because peak vertical GRF is

368   usually inversely associated with duty factor (Alexander 1984; Witte et al. 2004). Unfortunately

369   in giraffes it may not be possible to accurately predict peak GRF from duty factor alone. In our

370   previous work peak vertical GRF during walking was speed-independent; a finding which may

371   be related to limb compliance (Basu et al., under review). This could be explored in future with a

372   giraffe musculoskeletal model and a forward dynamics simulation in which peak GRFs are

373   simulated as a function of speed, as experimental data collection from giraffes galloping over

374   force plates may be logistically impossible. Such findings would have implications for muscle

375   power demands and tissue safety factors in giraffes.

376   Contralateral limb phase decreased with speed (Figure 7), resulting in a greater degree of overlap

377   between lead and non-lead footfalls. This is consistent with a peak GRF-minimising strategy,

378   where body weight is evenly distributed over two limbs during a greater proportion of the stride.

379   Such a mechanism would be particularly advantageous to giraffes, which possess a

380   disproportionately slender appendicular skeleton, and so may be sensitive to large skeletal

381   compressive and bending stresses (Biewener 1983; McMahon 1975).

382   The phase relationship between body pitch and neck angle was variable between trials, with a

383   mean congruity of 70%. Given that 100% congruity would represent in-phase neck ventroflexion

384   and positive body pitching, we speculate that the giraffe neck is inertially stabilised with respect

385   to a world frame, and is effectively decoupled from the motions of the trunk during running; a

386   similar situation to the energy-conserving mechanism observed during walking (Basu et al.). A

387   method of testing this idea in the future would be to examine the effect of ground incline, net

388   acceleration and high-speed turning on neck kinematics. Topography generated by the 3D terrain

389   mapping method used in this study would be particularly useful for this purpose. Alternatively,

390   the variation between strides with respect to phase, as well as the variation in neck angle (Figure

391   2B), may indicate an additional or different effect. Variation in angular neck kinematics during

392   galloping has also been noted by Dagg (Dagg 1962). Defining neck kinematics using a single

393   angle may partly explain this issue, as the cervical vertebral series is far from rigid, and displays

394   varying degrees of curvature over the course of a single stride (Video S1). A spline-based

395   analysis may yield a more robust parameter with which to investigate giraffes' neck kinematics.

396 The giraffes were studied in their natural habitat, meaning any conclusions can be more

397 confidently applied to giraffes as a wild species, compared with a laboratory setting where

398 conclusions are confined to a specific set of conditions. The drawback is that controlled

399 experimental conditions were not strictly possible. The effects of confounding variables were

400 kept to a minimum by only collecting data from relatively flat terrain, avoiding extremes of

401 weather conditions and comparing giraffes of similar size. Textured terrain models can be used

402 in future to quantify elevation, substrate type and other random effects. Such terrain parameters

403 may useful in investigating giraffes' athletic abilities and energetic costs.

404

405

CONCLUSIONS

407 This study was a novel application of a UAV system, and has highlighted the gains and technical

408 challenges of this method. We recommend that UAV users minimise kinematic measurement

409 error by maximising the focal distance and confining the study subject to the centre of the field

410 of view. Giraffes' lack of an intermediate gait was compensated for by their rotary galloping

411 gait; giraffes are slow gallopers. Duty factors were lower than predicted by dynamic similarity,

412 suggesting that galloping giraffes may experience high peak ground reaction forces. However, a

413 speed-dependent reduction in contralateral limb phase, and modest maximal speed may maintain

414 appropriate tissue safety factors.

415

ACKNOWLEDGEMENTS

423

424

REFERENCES

426

427   Ahn AN, Furrow E, and Biewener AA. 2004. Walking and running in the red-legged running
428   frog, Kassina maculata. *Journal of experimental Biology* 207:399-410.
429   10.1242/jeb.00761
430   Alexander R, and Jayes A. 1983. A dynamic similarity hypothesis for the gaits of quadrupedal
431   mammals. *Journal of Zoology* 201:135-152.
432   Alexander RM. 1984. The Gaits of Bipedal and Quadrupedal Animals. *The International Journal*
433   *of Robotics Research* 3:49-59. 10.1177/027836498400300205
434   Alexander RM, Langman VA, and Jayes AS. 1977. Fast locomotion of some African ungulates.
435   *Journal of Zoology* 183:291-300. 10.1111/j.1469-7998.1977.tb04188.x
436   Badlangana NA, JW; Manger, P. 2009. The giraffe cervical vertebral column: a heuristic
437   example in understanding evolutionary processes? *Zoological Journal of the Linnean*
438   *Society* 155:736-757.
439   Basu C, Wilson A, and Hutchinson JR. Under Review. The kinematics and ground reaction
440   forces of walking giraffes.
441   Benjamini Y, and Hochberg Y. 1995. Controlling the false discovery rate: a practical and
442   powerful approach to multiple testing. *Journal of the royal statistical society Series B*
443   *(Methodological)*:289-300.
444   Biewener AA. 1983. Allometry of quadrupedal locomotion: the scaling of duty factor, bone
445   curvature and limb orientation to body size. *Journal of experimental Biology* 105:147-
446   171.
447   Dagg AI. 1962. The Role of the Neck in the Movements of the Giraffe. *Journal of Mammalogy*
448   43:88-97. 10.2307/1376883
449   Dagg AI, and Vos Ad. 1968. The walking gaits of some species of Pecora. *Journal of Zoology*
450   155:103-110.
451   Daley MA, Channon AJ, Nolan GS, and Hall J. 2016. Preferred gait and walk–run transition
452   speeds in ostriches measured using GPS-IMU sensors. *Journal of experimental Biology*
453   219:3301-3308.
454   Dunbar DC. 2004. Stabilization and mobility of the head and trunk in vervet monkeys
455   (*Cercopithecus aethiops*) during treadmill walks and gallops. *Journal of experimental*
456   *Biology* 207:4427-4438.
457   Dunbar DC, Macpherson JM, Simmons RW, and Zarcades A. 2008. Stabilization and mobility of
458   the head, neck and trunk in horses during overground locomotion: comparisons with
459   humans and other primates. *Journal of experimental Biology* 211:3889-3907.
460   10.1242/jeb.020578
461   Hedrick TL. 2008. Software techniques for two- and three-dimensional kinematic measurements
462   of biological and biomimetic systems. *Bioinspir Biomim* 3:034001. 10.1088/1748-
463   3182/3/3/034001
464   Heglund NC, and Taylor CR. 1988. Speed, stride frequency and energy cost per stride: how do
465   they change with body size and gait? *Journal of experimental Biology* 138:301-318.
466   Hildebrand M. 1976. Analysis of tetrapod gaits: general considerations and symmetrical gaits.
467   *Neural control of locomotion* 18:203-206.
468   Hildebrand M. 1977. Analysis of Asymmetrical Gaits. *Journal of Mammalogy* 58. doi
469   10.2307_137957
470   Hubel TY, Myatt JP, Jordan NR, Dewhirst OP, McNutt JW, and Wilson AM. 2016. Additive
471   opportunistic capture explains group hunting benefits in African wild dogs. *Nature*
472   *communications* 7:11033.

473 Hutchinson JR, Schwerda D, Famini DJ, Dale RH, Fischer MS, and Kram R. 2006. The
474   locomotor kinematics of Asian and African elephants: changes with speed and size.
475   *Journal of experimental Biology* 209:3812-3827.
476 Larson SG, and Stern JT. 2006. Maintenance of above-branch balance during primate arboreal
477   quadrupedalism: Coordinated use of forearm rotators and tail motion. *American Journal*
478   *of Physical Anthropology* 129:71-81. 10.1002/ajpa.20236
479 Libby T, Moore TY, Chang-Siu E, Li D, Cohen DJ, Jusufi A, and Full RJ. 2012. Tail-assisted
480   pitch control in lizards, robots and dinosaurs. *Nature* 481:181-184.
481   http://www.nature.com/nature/journal/v481/n7380/abs/nature10710.html#supplementary-
482   information
483 Maxwell M. 1924. *Stalking big game with a camera in equatorial Africa: with a monograph on*
484   *the African elephant*: The Century Co.
485 McMahon TA. 1975. Allometry and biomechanics: limb bones in adult ungulates. *The American*
486   *Naturalist* 109:547-563.
487 Rasband W. 2009. ImageJ; US National Institutes of Health: Bethesda, MD, 1997-2006.
488 Starke SD, and Clayton HM. 2015. A universal approach to determine footfall timings from
489   kinematics of a single foot marker in hoofed animals. *PeerJ* 3:e783.
490 Tao W, Liu T, Zheng R, and Feng H. 2012. Gait analysis using wearable sensors. *Sensors*
491   12:2255-2283.
492 Wilson AM, Lowe JC, Roskilly K, Hudson PE, Golabek KA, and McNutt JW. 2013.
493   Locomotion dynamics of hunting in wild cheetahs. *Nature* 498:185-189.
494   10.1038/nature12295
495 http://www.nature.com/nature/journal/v498/n7453/abs/nature12295.html#supplementary-
496   information
497 Witte T, Knill K, and Wilson A. 2004. Determination of peak vertical ground reaction force from
498   duty factor in the horse (*Equus caballus*). *Journal of experimental Biology* 207:3639-
499   3648.
500
501

Table 1(on next page)

Details of study sites

1

	Size (hectares)	Number of giraffes	Giraffe temperament	Calibration methods used
Site 1	460	2	Tame	A,B,C
Site 2	250	6	Wild	C
Site 3	12500	27	Wild	C

2

Table 2(on next page)

Comparison of MTP-C distance estimates from one giraffe in field site 1.

Method A resulted in the lowest standard deviation, and was used as the standard to which the other methods were compared. Method C was compared twice; once using artificial ground markers, once using naturally occurring features.

Method	Range (m)	MTP-C distance estimate		
		Mean (m)	Standard deviation (m)	% error
A	0.78 - 0.84	0.814	0.018	
B	0.76 - 0.82	0.783	0.022	3.7
$C_{natural}$	0.74 - 0.88	0.850	0.099	4.9
$C_{artificial}$	0.76 - 0.83	0.784	0.024	3.7

1

Table 3 (on next page)

Comparison of power equations from the current dataset, with equations for dynamic similarity.

Data from Alexander and Jayes (1983) were digitised, with the exception of hind duty factor (*) which was not presented as a figure. Equations are in the form $y = a(Fr)^b$. The ± 95% confidence interval is given in brackets where available. Relative stride length (stride length / leg length) in giraffes was consistent with the predictions for dynamic similarity; i.e. giraffes take proportionally similar strides. Fore and hind duty factors in giraffes were lower than predicted by dynamic similarity, as indicated by the significantly lower coefficient (a).

Stride parameter	Giraffe coefficients		Coefficients from Alexander and Jayes 1983	
	a	b	a	b
Relative stride length	1.98 (0.11)	0.31 (0.11)	1.85 (0.09)	0.43 (0.02)
Fore duty factor	0.44 (0.01)	-0.17 (0.06)	0.52 (0.02)	-0.27 (0.04)
Hind duty factor	0.41 (0.01)	-0.19 (0.07)	0.53*	-0.28 (0.03)*

1

Figure 1

A comparison of features from UAV footage, a 3D textured mesh and a photograph.

(A) Still frame of a galloping giraffe from UAV video. (B) Render from a textured 3D mesh, created from aerial photographs. The natural feature from the still image can be referenced to the textured 3D mesh. The feature was measured in the same plane as the hindlimb, and this measurement used to convert the MTP-C pixel distance (C) into an estimation of the metric distance.
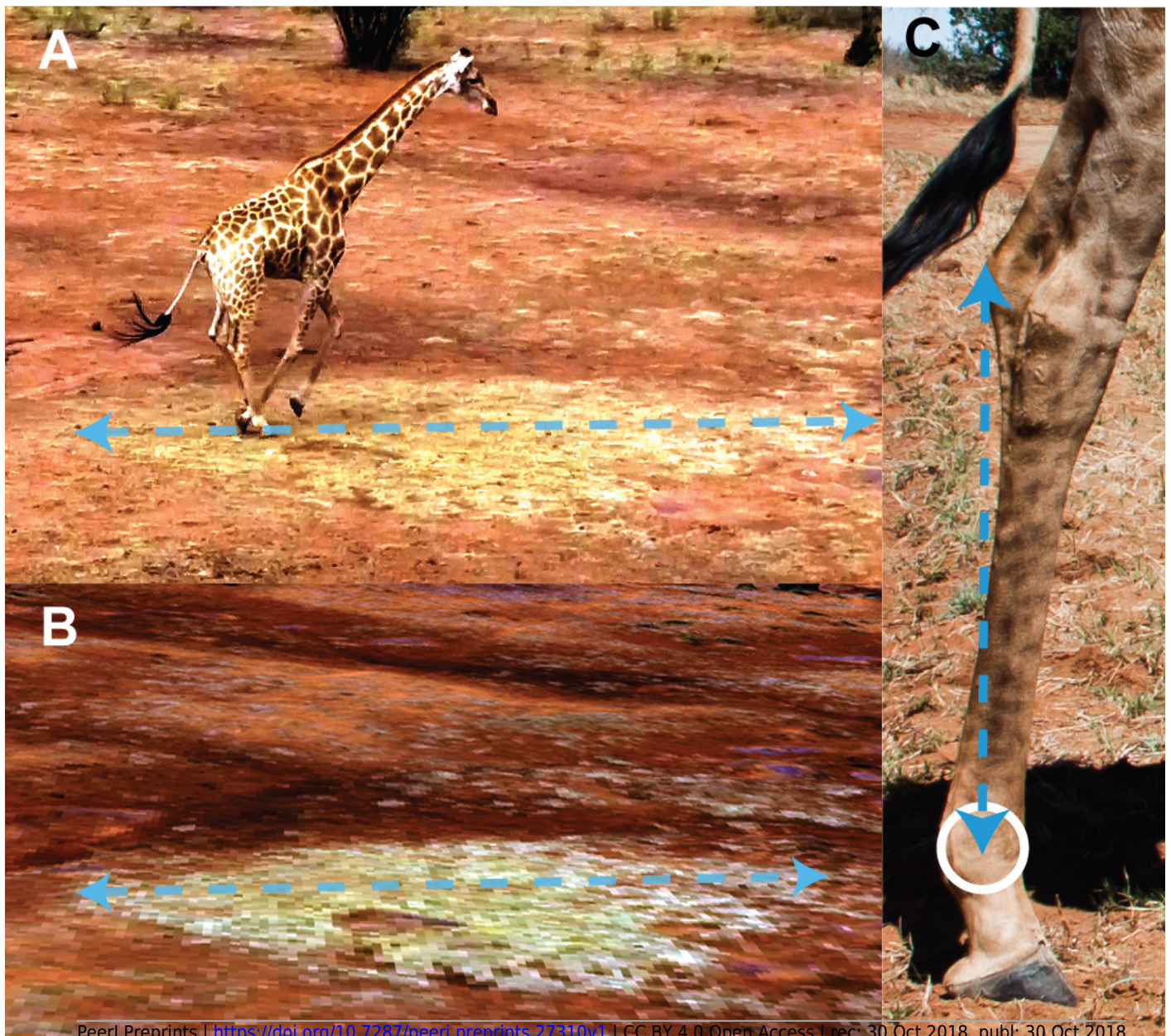
Figure 2

Neck and pitch angle time series during steady state rotary galloping

(A) The anatomical definitions of neck angle and body pitch, demonstrated in a standing individual. Neck angle (B) and body pitch (C) time series from strides commencing with foot-ground contact by the non-leading hindlimb, with mean time series (thicker line).
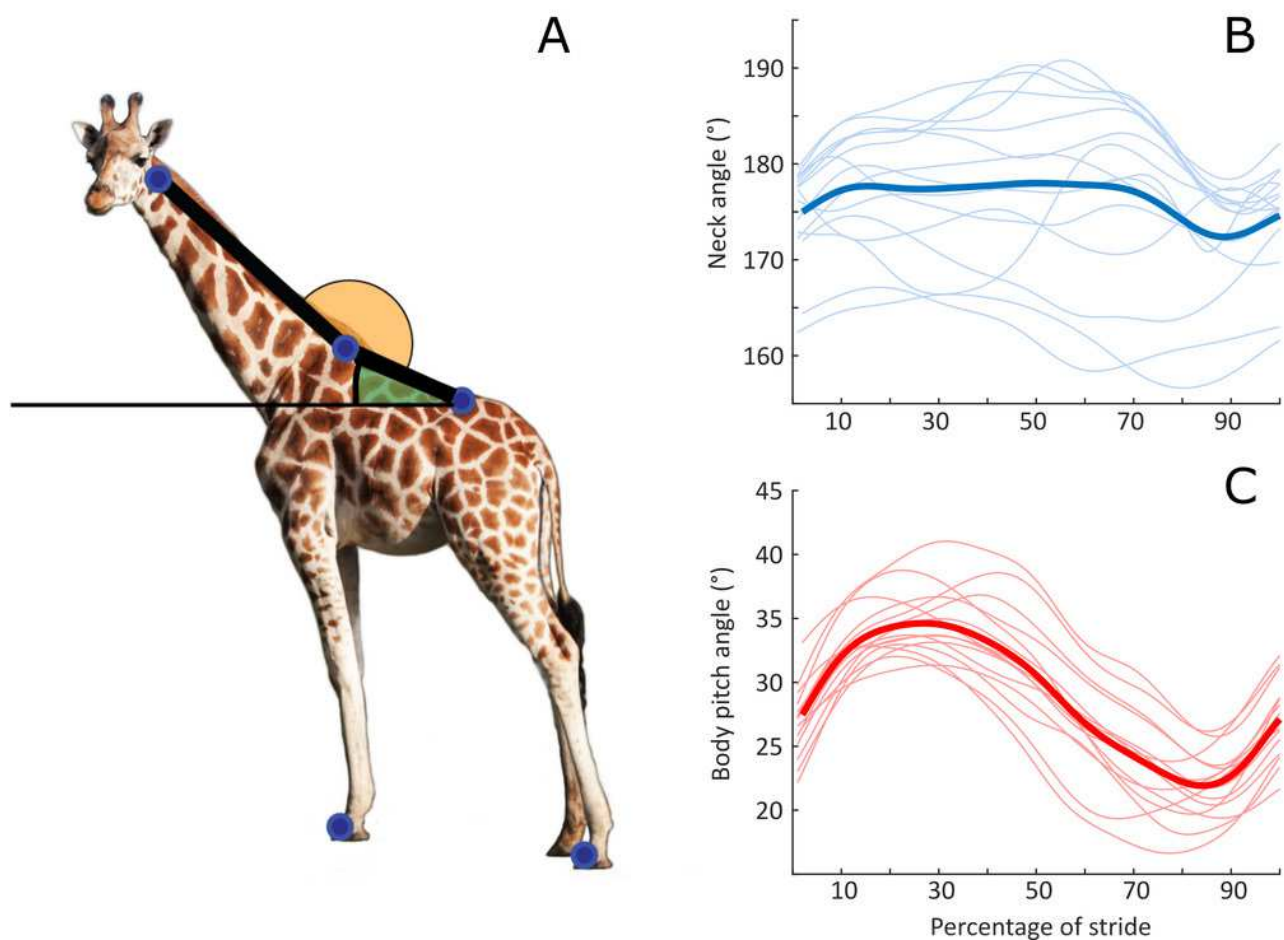
Figure 3(on next page)

Box and whisker plot showing percentage error of UAV derived speed measurements compared to treadmill speed, with overlying data points.

Human running speed measured by the UAV was most accurate when the subject was furthest distance, and when they were centred in the field of view.
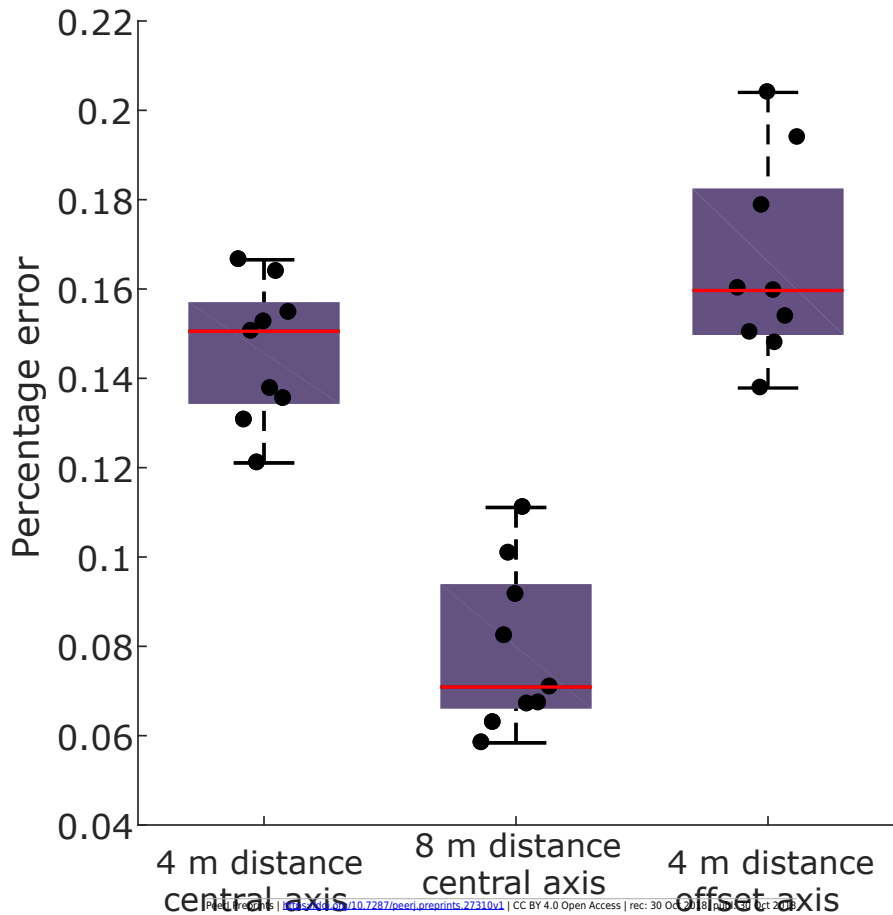
Figure 4(on next page)

Footfall sequence of a representative stride from a giraffe running at 4.88 ms⁻¹, with a forelimb duty factor of 0.39 and hindlimb duty factor of 0.38.
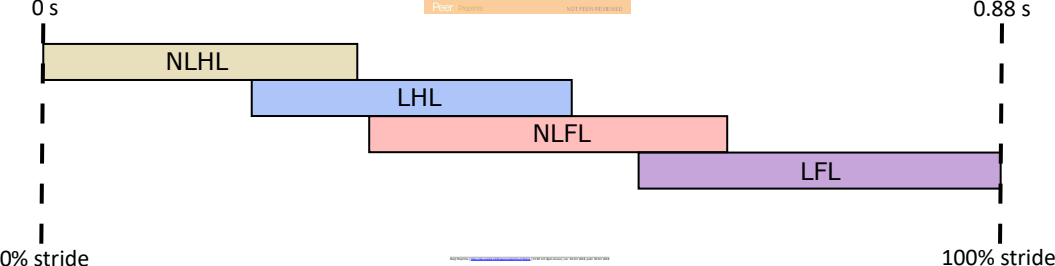
0 s   0.88 s

NLHL

LHL

NLFL

LFL

0% stride   100% stride

Figure 5(on next page)

Change in stride length (m) and stride frequency (Hz) as a function of speed (ms^{-1})

Stride length (A) changed by 0.55 m per unit of speed (u): y = 0.55u + 1.43, R^2 = 0.63, p < 0.001. Stride frequency (B) changed by 0.05 Hz for every unit of speed (u): y = 0.05u + 0.88, R^2 = 0.66, p < 0.001.
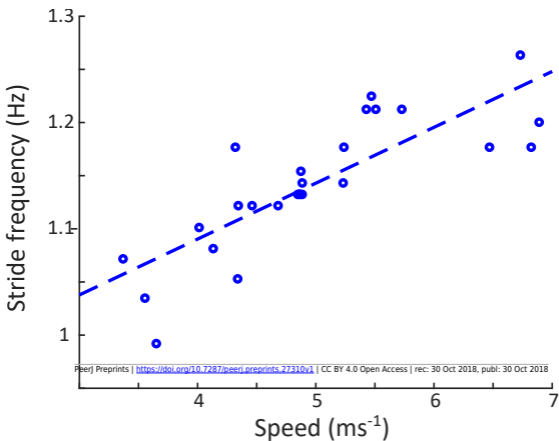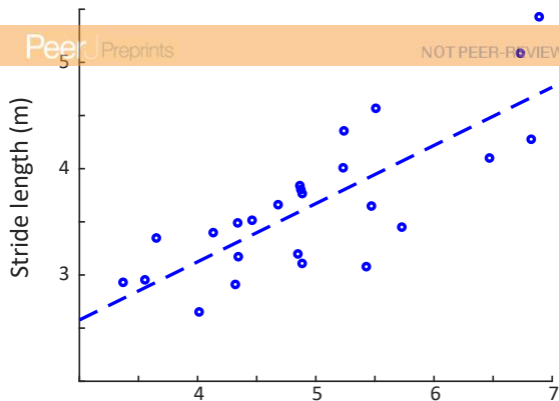
Figure 6(on next page)

Changes in stance duration (s), swing duration (s) and duty factor as a function of speed (ms^{-1})

(A) Stance duration was longer in the forelimb (blue circles) than the hindlimb (red circles), and both decreased with speed (FL: y = - 0.04u + 0.57, R^2 = 0.70, p < 0.001; HL: y = - 0.04u + 0.55, R^2 = 0.74, p < 0.001). Swing duration (B) was independent of speed, resulting in a duty factor (C) which was greater in the forelimb than the hindlimb, and which decreased with speed (FL: y = -0.03u + 0.55, R^2 = 0.49, p < 0.001; HL: y = -0.03u + 0.53, R^2 = 0.54, P < 0.001).
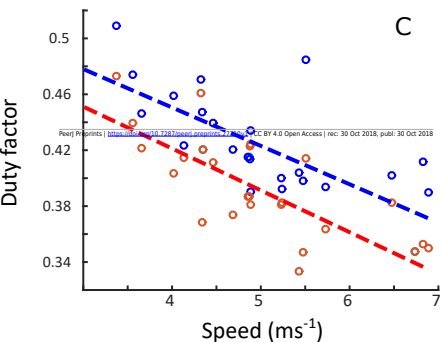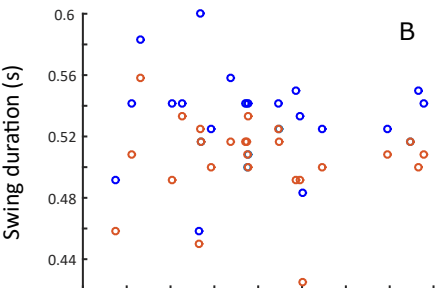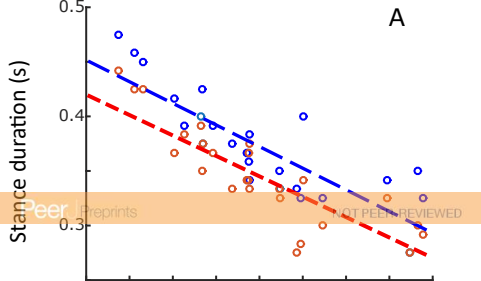
Figure 7(on next page)

Changes in contralateral limb phase as a function of speed (ms^{-1})

Contralateral limb phase is expressed as the relative lag time between footfalls of the left and right side. Phase was greater in the forelimb than the hindlimb, and decreased with speed. A decrease in phase indicated that the overlap between left and right footfalls was greater at faster speeds (FL: -0.01u + 0.36, R^2 = 0.35, p = 0.002; HL: y = -0.02u + 0.29, R^2 = 0.57, p < 0.001).
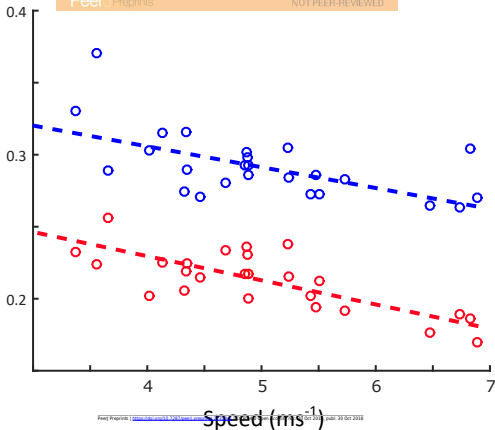
Figure 8

A still image of a rotary galloping giraffe taken from video footage recorded using a DJI Phantom 4 UAV, at study site 3.

We recommend that kinematic analyses of the study subject is confined to the centre box of a 3x3 grid, overlying the field of view. Linear and angular measurements outside of this area will be subject to greater parallax error.